RESEARCH ARTICLE

WILEY

Neuropsychiatric symptoms associated multimodal brain networks in Alzheimer's disease

Kaicheng Li[1,2] | Qingze Zeng[1] | Xiao Luo[1] | Shile Qi[3] | Xiaopei Xu[1] | Zening Fu[2] | Luwei Hong[1] | Xiaocao Liu[1] | Zheyu Li[4] | Yanv Fu[4] | Yanxing Chen[4] | Zhirong Liu[4] | Vince D. Calhoun[2,5,6] | Peiyu Huang[1] | Minming Zhang[1]

[1]Department of Radiology, The Second Affiliated Hospital of Zhejiang University School of Medicine, Hangzhou, China

[2]Tri-Institutional Center for Translational Research in Neuroimaging and Data Science (TReNDS): Georgia State University, Georgia Institute of Technology, and Emory University, Atlanta, Georgia, USA

[3]Department of Computer Science and Engineering, Nanjing University of Aeronautics and Astronautics, Nanjing, China

[4]Department of Neurology, The Second Affiliated Hospital of Zhejiang University School of Medicine, Hangzhou, China

[5]Department of Psychology, Computer Science, Neuroscience Institute, and Physics, Georgia State University, Atlanta, Georgia, USA

[6]Department of Electrical and Computer Engineering, Georgia Institute of Technology, Atlanta, Georgia, USA

Correspondence
Minming Zhang and Peiyu Huang, Department of Radiology, The Second Affiliated Hospital of Zhejiang University School of Medicine, No. 88 Jie-Fang Road, Shang-Cheng District, Hangzhou 310009, China.
Email: zhangminming@zju.edu.cn (M. Z.) and huangpy@zju.edu.cn (P. H.)

Abstract

Concomitant neuropsychiatric symptoms (NPS) are associated with accelerated Alzheimer's disease (AD) progression. Identifying multimodal brain imaging patterns associated with NPS may help understand pathophysiology correlates AD. Based on the AD continuum, a supervised learning strategy was used to guide four-way multimodal neuroimaging fusion (Amyloid, Tau, gray matter volume, brain function) by using NPS total score as the reference. Loadings of the identified multimodal patterns were compared across the AD continuum. Then, regression analyses were performed to investigate its predictability of longitudinal cognition performance. Furthermore, the fusion analysis was repeated in the four NPS subsyndromes. Here, an NPS-associated pathological–structural–functional covaried pattern was observed in the frontal-subcortical limbic circuit, occipital, and sensor-motor region. Loading of this multimodal pattern showed a progressive increase with the development of AD. The pattern significantly correlates with multiple cognitive domains and could also predict longitudinal cognitive decline. Notably, repeated fusion analysis using subsyndromes as references identified similar patterns with some unique variations associated with different syndromes. Conclusively, NPS was associated with a multimodal imaging pattern involving complex neuropathologies, which could effectively predict longitudinal cognitive decline. These results highlight the possible neural substrate of NPS in AD, which may provide guidance for clinical management.

KEYWORDS
Alzheimer's disease, cognitive decline, frontal-subcortical limbic circuit, neuropsychiatric symptoms, supervised multimodal fusion

1 | INTRODUCTION

Neuropsychiatric symptoms (NPS) are frequently observed in mild cognitive impairment (MCI) and Alzheimer's disease (AD) (Lyketsos et al., 2002; Lyketsos et al., 2011), with 80% of AD patients involved (Lyketsos et al., 2002). Longitudinal studies showed that concomitant NPS is associated with accelerated cognitive decline (Fischer et al., 2012; Karttunen et al., 2011; Teng et al., 2007), severer neurodegeneration (Scaricamazza et al., 2019), and an earlier death (Peters et al., 2015). Accordingly, exploring the underlying pathophysiology correlates of NPS in AD is crucial for improving clinical management.

Previous neuroimaging studies have revealed NPS-related brain abnormalities from different aspects, suggesting that NPS is associated with brain functional and structural impairments in the cortical and subcortical limbic circuit. For instance, depression has been found associated with gray matter (GM) atrophy, white matter (WM) lesion, and cortical hypometabolism (Chen et al., 2021). AD neuropathologies are also associated with NPS (Ehrenberg et al., 2018; Krell-Roesch et al., 2019), although the specific contribution of different pathologies is still unclear. Some studies ascribe NPS to Tau pathology (Tissot et al., 2021), but some others highlighted the importance of Aβ burden (Pichet Binette et al., 2021). Apparently, these brain abnormalities involve complex neuropathologies which may inherently interplay with each other. For example, Aβ (Buckner et al., 2005; Kvavilashvili et al., 2020; Mormino et al., 2011) accumulation could promote Tau (Buckner et al., 2008) pathology, causing further functional and structural impairments. Nevertheless, they may also independently develop based on different genetic and environmental factors. Therefore, when investigating their impacts on clinical function, it is important to use methods that can incorporate both complementary multimodal information and cross-modal associations.

Recently, a reference-guided multimodal fusion method, called multisite canonical correlation analysis with reference + joint independent component analysis (MCCAR + jICA) (Qi et al., 2018), was proposed to identify covarying multimodal imaging patterns that correlate with a specific disease trait, such as NPS. Specifically, MCCAR + jICA uses subject-wise clinical measure as a reference to supervise multimodal image fusion by maximizing both inter-modality association and reference-modality correlation. Thus, this model can effectively extract multimodal patterns associated with a specific disease trait, taking inter-modality associations into account. Previous application of this method successfully revealed cognitive-related networks in schizophrenia (Sui et al., 2018) and electroconvulsive therapy treatment responsive networks in depression (Qi et al., 2020). Accordingly, we believe that the MCCAR + jICA model is a proper method for comprehensively evaluating the neuroimaging phenotypes of NPS in AD-continuum subjects.

In the present study, we focused on four goals: (1) identify multimodal brain patterns associated with NPS total score within AD continuum; (2) assess group differences of these identified regions; (3) evaluate ability of the identified brain patterns to predict changes in cognition; and (4) identify the common and unique multimodal attributes among four neuropsychiatric subsyndromes (psychosis, affective symptoms, hyperactivity, apathy).

2 | MATERIALS AND METHODS

2.1 | Study participants

Data used in the current study were obtained from the AD neuroimaging initiative (ADNI) database (Supplementary Material 1 provides detailed information about ADNI). All included subjects underwent the T1-weighted structural scan, $[^{18}F]$-AV45 PET, $[^{18}F]$-AV1451 PET, resting-state functional MRI (rsfMRI), NPS score, and comprehensive neuropsychological assessments (Supplementary Material 2 provides detailed information about the MRI and PET acquisition). This criterion yielded 167 healthy control (HC), 34 subjective memory complaint (SMC), 118 MCI, and 18 AD patients from the ADNI database (see flowchart and inclusion criteria in Supplementary Material 3).

2.2 | Neuropsychological assessment

All subjects completed comprehensive neuropsychological tests, including assessment of general mental status (MMSE and CDR), memory (ADNI memory composite score [ADNI-MEM]), executive function (ADNI executive function composite score [ADNI-EF]), language function (ADNI language function composite score [ADNI-LAN]), and visuospatial function (ADNI visuospatial function composite score [ADNI-VS]). More detailed information about composite cognitive scores is provided in Supplementary Material 4.

2.3 | Neuropsychiatric assessment

Quantitative assessment of behavioral manifestations was performed via the Neuropsychiatric Inventory (NPI) (Cummings, 1997). The NPI is a validated caregiver-based questionnaire for NPS evaluation in patients with dementia (Cummings, 1997). It assesses the frequency (from 0 to 4) and severity (from 0 to 3) of 12 NPSs: delusions, hallucinations, agitation/aggression, dysphoria/depression, anxiety, euphoria/elation, apathy/indifference, disinhibition, irritability, aberrant motor behavior, nighttime sleep disturbances, and appetite/eating changes. The maximum total score (frequency × severity) for each NPS is 12, and the NPI total cumulative score is 144 (Cummings, 1997). Detailed information of the 12 NPI items was listed in Supplementary Material 5.

Based on previous studies (Aalten et al., 2007; Ballarini et al., 2016), we further clustered the 12 NPI symptoms into 4 distinct subsyndromes as follows: (1) psychosis (delusions, hallucinations, and nighttime sleep disturbances); (2) affective symptoms (anxiety and depression); (3) hyperactivity (agitation/aggression, irritability, euphoria/elation, aberrant motor behavior, and disinhibition); and (4) apathy (apathy and eating and appetite changes). The score for each

subsyndrome was derived by multiplying the frequency and severity of the symptom.

2.4 | Image preprocessing

RsfMRI data preprocessing was performed using the data processing assistant and resting-state fMRI toolbox (DPARSF; www.rfmri.org/dpasfa) (Chao-Gan & Yu-Feng, 2010) based on Statistical Parametric Mapping 12 (SPM12; www.fil.ion.ucl.ac.uk/spm). The first five rsfMRI scans were discarded for the signal equilibrium and the subject's adaptation to the scanning noise (Chao-Gan & Yu-Feng, 2010). The remaining 135 images were corrected for timing differences in slice acquisition. After that, a rigid body motion correction was performed to correct the head motion of the fMRI scans. Then, the mean rsfMRI image was co-registered to the subject-specific T1 image, spatially normalized to the Montreal Neurological Institute (MNI) standard space, and resampled into $3 \times 3 \times 3$ mm^3 cubic voxel. Scrubbing was then performed to reduce motion-related artifacts by using a frame-wise displacement threshold of 0.5 (Power et al., 2012). To control the residual effects of motion and other nonneuronal factors, we removed covariates, including six head motion parameters and signals of WM and cerebrospinal fluid (CSF) (Chao-Gan & Yu-Feng, 2010; Friston et al., 1996). The fMRI data were then smoothed using an 8 mm full width at half maximum Gaussian kernel (FWHM). Finally, we calculated the amplitude of the low frequency fluctuation (ALFF) measure, which was the average square root of the power spectrum (across 0.01–0.1 Hz) (Zang et al., 2007).

The preprocessing steps for T1-weighted image were: (1) spatial registration to a reference brain template; (2) tissue segmentation into GM, WM, and CSF based on an adaptive maximum a posterior approach with partial volume estimation. An iterative hidden Markov random field model (Cuadra et al., 2005) was further applied to remove isolated/unclassified voxels; (3) bias correction of intensity nonuniformities; (4) the GM maps were normalized to MNI coordinate space, modulated via the Jacobian, and resampled to $3 \times 3 \times 3$ mm^3 voxel size; and (5) the GM volume (GMV) maps were smoothed using an 8 mm FWHM Gaussian kernel.

The [18F]-AV45 PET and [18F]-AV1451 PET preprocessing was performed using the PET-PVE12 (an SPM toolbox for partial volume effects (PVE) correction in brain PET (Gonzalez-Escamilla et al., 2017)). Briefly, the T1-weighted image was processed using the same method described above. Then, [18F]-AV45 PET and [18F]-AV1451 PET data were co-registered to the structural MRI data and corrected for PVE using the voxel-wise method defined by Muller-Gartner et al. (PVEc-MG) methods (Muller-Gartner et al., 1992). Here, we set the isotropic point spread function at 8 mm according to the effective image resolution of the ADNI PET data. Then, the voxel-wise [18F]-AV45 PET map was calculated using the whole cerebellar signal in the individual raw PET images as the reference, and the voxel-wise [18F]-AV1451 SUVR map was calculated using cerebellum crus. Finally, for voxel-based analyses, PVEc-MG corrected [18F]-AV45 PET and [18F]-AV1451 PET images

were spatially warped using the deformation fields derived from registration of the co-registered MRI scans to the reference template. Finally, warped images were smoothed with an 8 mm FWHM Gaussian kernel.

2.5 | Feature extraction

Four representative neuroimaging features ([18F]-AV45 PET SUVR, [18F]-AV1451 PET SUVR, GMV, and ALFF) were included as the input of fusion analysis. Here, we used the [18F]-AV45 PET SUVR and [18F]-AV1451 PET SUVR to reflect AD neuropathologies, volume changes to reflect the GM atrophy, and ALFF to reflect the intrinsic brain activity. Normalization is done separately for each feature using the square root of mean of squared data for all subjects.

2.6 | Multimodal fusion using NPS as the reference

The normalized features were jointly analyzed based on MCCAR + jICA (Qi et al., 2018) using the Fusion ICA Toolbox (FIT, https://trendscenter.org/software/fit/). Figure 1 shows a detailed analysis flowchart. First, for each modality, the neuroimaging features were stacked to 2D matrices with the row indicates the subject and the column indicates the features. Then, NPS total score was used as the reference to guide the joint decomposition of four features to generate spatial maps and their corresponding canonical variants for each modality. Based on the modified minimum description length criterion (Li et al., 2007), 10 components were estimated for each feature. MCCAR identifies joint multimodal components that show maximal correlation with the reference and inter-modality covariation based on supervised learning. Finally, jICA is applied to the concatenated spatial maps to obtain the final independent components (ICs) and their corresponding mixing matrices. Here, the ICs represent the spatial location correlates with reference, while the loading in mixing matrices represents the contribution weight for each subject in the corresponding component. More details of the model are shown in Qi et al. (2018).

Analysis of variance (ANOVA) was performed to explore group differences in the loadings of the four imaging features. Post hoc analysis using pair-wise two-sample t tests was performed to examine the source of ANOVA difference (significant at $p < .05$, false discovery rate [FDR] corrected). We listed the detailed analysis flowchart in Figure 1.

2.7 | Correlation between imaging features and cognitive scores

To explore whether the multimodal brain alterations underpin the cognitive decline, we further examined the potential relationship between loadings of imaging features and cognitive performance. The Pearson correlation between the loadings of imaging features and

(a)
Fusion with NPS total score as the reference

(b)
Associations between identified multimodal pattern and cognition

(c)
Fusion with NPS subsyndrome score as the reference
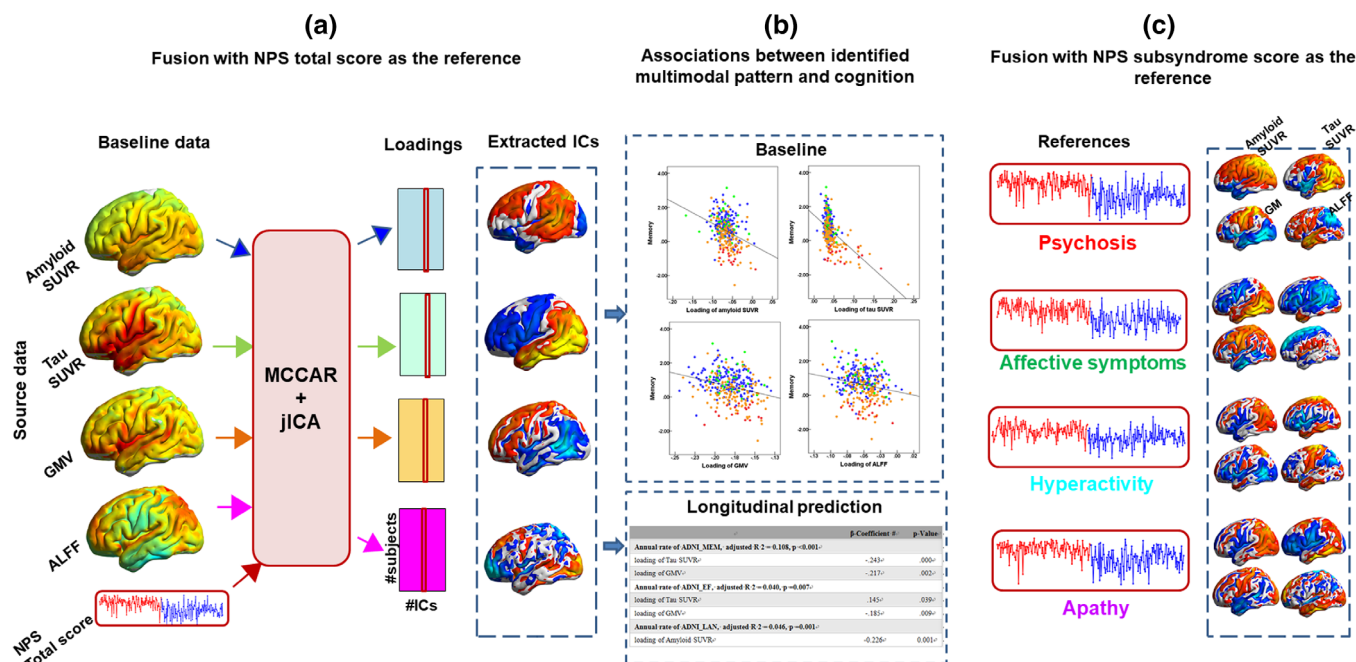
FIGURE 1 Flowchart of NPS-guided multimodal fusion and prediction analysis. (a) NPS total score was set as the reference to guide the four-way MRI fusion. (b) Correlation analysis and linear regression were performed to estimate the associations between the identified multimodal pattern and baseline cognitive performance across groups and longitudinal cognitive scores in the subgroup, respectively. (c) The same fusion with reference method was performed by using four subsyndrome scores as the reference individually, to guide the four-way MRI fusion to further identify the common and unique multimodal attributes. ALFF, amplitude of low frequency fluctuations; GMV, gray matter volume; IC, independent components; ICA, independent component analysis; MCCAR, multisite canonical correlation analysis with reference; NPS, neuropsychiatric symptoms; SUVR, standard uptake value ratios

cognitive scores (ADNI-MEM, ADNI-EF, ADNI-LAN, ADNI-VS) was calculated across subjects (significant at $p < .05$, FDR corrected).

2.8 | Predictability of the identified pattern on the longitudinal cognition progression

We also tested the predictability of the identified pattern on longitudinal cognitive changes in the subgroups (HC = 80, SMC = 30, MCI = 80, AD = 9). For each domain score, simple linear regression analyses were performed using all subjects. Annual change rate of the cognitive score was set as the dependent variable, and the loadings of the four imaging features were regressors, with age, gender, and education as covariates. For comparison, the predictability of NPS total score was also investigated with similar settings.

2.9 | Multimodal fusion using each neuropsychiatric subsyndrome as the reference

To further identify the common and unique multimodal covarying patterns in four neuropsychiatric subsyndromes (psychosis, affective symptoms, hyperactivity, apathy), the same fusion analysis method was performed using each subsyndrome score as a reference, respectively.

3 | RESULTS

3.1 | Demographic and neuropsychological data

Detailed demographics are provided in Table 1. We used a chi-squared test for categorical (gender, APOE genotype) and ANOVA for continuous data (age, education), respectively (SPSS, version 19.0). Then, a two-sample t test was performed to reveal the source of ANOVA difference (significant at $p < .05$).

There were no group differences in age, gender, or education among HC, SMC, MCI, and AD. In terms of cognitive level, MCI and AD had lower cognitive scores in all items compared to HC. In terms of neuropsychiatric scores, MCI and AD had higher NPS total scores and subsyndromes scores compared to HC. SMC showed increased affective symptoms when compared to HC. Moreover, comparisons between patient groups (SMC, MCI, and AD) showed progressively decreased cognitive scores and increased NPS scores.

3.2 | NPS total score associated multimodal covarying imaging pattern

One joint component was significantly correlated with NPS total score and showed significant alterations along the AD continuum (HC, SMC, MCI, AD). The resulting spatial maps were Z-transformed and

TABLE 1 Demographic information

Demographic characteristics	HC $n = 167$	SMC $n = 34$	MCI $n = 118$	AD $n = 18$	F-value/X^2	Significance
Age	74.85 ± 7.83	74.72 ± 4.85	75.35 ± 8.02	76.74 ± 8.55	0.40	.752
Gender (female)	95/167	23/34	51/118	6/18	11.09	.011[bcd]
Education	16.62 ± 2.47	16.47 ± 2.44	16.32 ± 2.79	15.28 ± 2.54	1.57	.196
Cognition						
CDR global	0.04 ± 0.13	0.09 ± 0.19	0.51 ± 0.39	0.89 ± 0.37	110.39	<.001[bcde]
CDR sum	0.14 ± 0.49	0.26 ± 0.59	2.07 ± 2.42	4.78 ± 1.93	74.17	<.001[bcde]
MMSE	28.92 ± 1.35	29.15 ± 1.05	27.03 ± 3.42	22.44 ± 2.43	51.64	<.001[bcde]
ADNI_MEM	0.93 ± 0.61	1.08 ± 0.73	0.26 ± 0.85	−0.88 ± 0.39	51.02	<.001[bcde]
ADNI_EF	0.96 ± 0.81	1.11 ± 0.82	0.26 ± 1.02	−0.91 ± 0.91	33.24	<.001[bcde]
ADNI_LAN	0.83 ± 0.76	1.00 ± 0.73	0.15 ± 1.01	−0.70 ± 0.63	30.15	<.001[bcde]
ADNI_VS	0.23 ± 0.63	0.03 ± 0.71	−0.10 ± 0.87	−0.70 ± 1.28	10.13	<.001[bce]
NPI score						
Total score	1.38 ± 3.28	3.62 ± 8.78	5.44 ± 9.37	10.72 ± 13.41	13.407	<.001[bce]
Hyperactivity	0.31 ± 1.09	1.24 ± 4.21	1.86 ± 3.92	4.17 ± 6.63	11.361	<.001[bce]
Psychosis	0.47 ± 1.46	0.71 ± 1.64	1.20 ± 2.29	1.56 ± 3.58	4.133	.007[bce]
Affective symptoms	0.37 ± 1.12	1.38 ± 3.22	1.04 ± 2.22	1.44 ± 2.23	5.223	.002[abc]
Apathy	0.23 ± 1.43	0.29 ± 1.40	1.34 ± 3.34	3.56 ± 5.76	11.376	<.001[bcde]

Note: Data are presented as means ± standard deviations. a–e denotes post hoc analysis further revealed the source of ANOVA difference (a: HC vs. SMC; b: HC vs. MCI; c: HC vs. AD; d: SMC vs. MCI; e: MCI vs. AD).

Abbreviations: AD, Alzheimer's disease; ADNI-EF, the composite scores for executive function in ADNI; ADNI-LAN, the composite scores for language in ADNI; ADNI-MEM, the composite scores for memory in ADNI; ADNI-VS, the composite scores for visuospatial function in ADNI; APOE, apolipoprotein; CDR, clinical dementia rating; GDS, geriatric depression scale; HC, healthy control; MCI, mild cognitive impairment; MMSE, Mini-Mental State Examination; NPI, Neuropsychiatric Inventory; SMC, subjective memory complaint.

visualized at |Z| > 2 in Figure 2(a). Along AD-continuum, NPS was correlated with (1) increased amyloid and Tau deposition while decreased GMV and ALFF in the inferior parietal gyrus (IPG); (2) increased Tau deposition while decreased GMV and amyloid deposition in the temporal regions (especially involves the HP); (3) decreased GMV, amyloid, and Tau deposition in the subcortical regions, including the insula and thalamus; and (4) increased ALFF in the occipital lobe while decreased ALFF in the frontal regions. Anatomical information for the identified regions in the joint component is listed in Supplementary Material 6.

As shown in Figure 2(b), higher loadings of imaging features were associated with worse NPS ($r = .18$, $p = .001$ for amyloid SUVR; $r = .21$, $p < .001$ for Tau SUVR; $r = .15$, $p = .006$ for GMV; $r = .13$, $p = .019$ for ALFF; p values are FDR corrected). Significant differences in loadings of amyloid SUVR, Tau SUVR, ALFF, and GMV (Figure 2(c)) among groups were also observed. To be specific, AD showed higher loadings than HC in amyloid SUVR, Tau SUVR, and GMV. MCI showed higher loadings than HC in Tau SUVR and GMV. Moreover, progressively increased loadings of amyloid SUVR, Tau SUVR, and GMV changes can be observed along the whole AD continuum.

Moreover, there were significant associations between loadings of imaging features: $r = .34$, $p < .001$ for association between amyloid SUVR and Tau SUVR; $r = .20$, $p < .001$ for association between amyloid SUVR and GMV; $r = .16$, $p = .003$ for association between amyloid SUVR and ALFF; $r = .19$, $p < .001$ for association between Tau

SUVR and GMV; $r = .15$, $p = .006$ for association between Tau SUVR and ALFF.

3.3 | Correlation between multimodal patterns and cognition

The identified multimodal brain alterations were significantly associated with cognitive performance in four major domains. The loadings of four imaging features (amyloid SUVR, Tau SUVR, ALFF, and GMV) were negatively correlated with memory, executive, language, and visuospatial function. Detailed results are listed in Table 2 and Figure 3.

We also performed the correlation analysis within every group (HC, SMC, MCI, and AD) and listed the results in Supplementary Material 7.

3.4 | Predictability of longitudinal cognition change

Linear regression analyses were performed in subgroups (NC = 80, SMC = 30, MCI = 80, AD = 9, detailed demographic information was listed in Supplementary Material 8). Our analysis found that the baseline multimodal changes can effectively predict the decline of
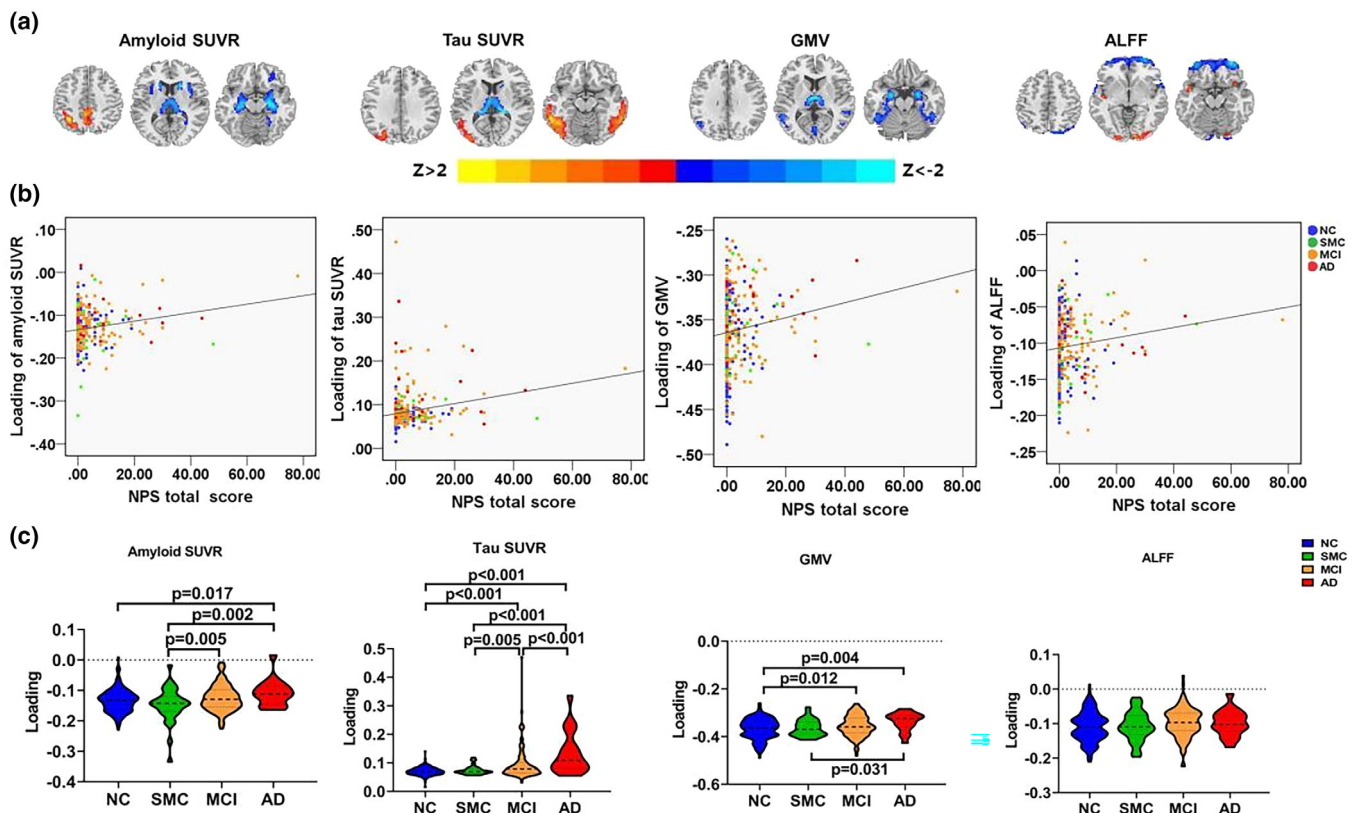
FIGURE 2 The identified joint component using NPS total score as the reference. (a) The spatial maps are visualized at |Z| > 2, where the positive Z-values (red regions) mean more amyloid and Tau deposition, higher GMV, and ALFF, and negative Z-values (blue regions) indicate less amyloid and Tau deposition, decreased GMV and ALFF. (b) The loadings of the identified imaging features and NPS total score were positively correlated (HC: blue dots, SMC: green dots; MCI: orange dots; AD: red dots). (c) Boxplot of the loading parameters of the identified joint component (FDR corrected). AD, Alzheimer's disease; ALFF, fractional amplitude of low frequency fluctuations; GMV, gray matter volume; HC, healthy control; MCI, mild cognitive decline; NPS, neuropsychiatric symptoms; SMC, subjective memory complaint; SUVR, standard uptake value ratios

TABLE 2 Correlation between loadings of the imaging features and cognitive scores in all subjects

Cognitive scores	Amyloid SUVR		Tau SUVR		GMV		ALFF	
	r	p	r	p	r	p	r	p
Memory	−.314	<.001*	−.533	<.001*	−.277	<.001*	−.202	<.001*
Executive function	−.329	<.001*	−.477	<.001*	−.295	<.001*	−.139	.012*
Language	−.164	.003*	−.469	<.001*	−.267	<.001*	−.188	.001*
Visuospatial function	−.233	<.001*	−.419	<.001*	−.140	.010*	−.040	.465

Note: The significant correlation that passes the multiple comparisons is marked by one asterisk (FDR corrected, $q = 0.05$).
Abbreviations: ALFF, amplitude of low frequency fluctuations; GMV, gray matter volume; SUVR, standard uptake value ratios.

follow-up memory, executive, and language functions. The baseline loadings of Tau SUVR and GMV were significantly correlated with the annual change rate of memory. The baseline loading of GMV was significantly correlated with the annual change rate of executive function; the baseline loading of amyloid SUVR was significantly correlated with the annual change rate of language (Table 3). Baseline NPS total score could not predict the longitudinal cognitive changes. Moreover, we also tested the predictability of the identified pattern on the longitudinal cognitive progression within each group (Supplementary Material 9).

3.5 | Imaging patterns associated with the four subsyndromes

Subsyndrome scores (psychosis, affective symptoms, hyperactivity, and apathy) associated joint components were also identified (Figure 4 and Supplementary Material 10). The NPS total score-associated and subsyndrome-associated multimodal patterns are displayed in Figure 4 for visual comparison. Both common and unique patterns were identified.
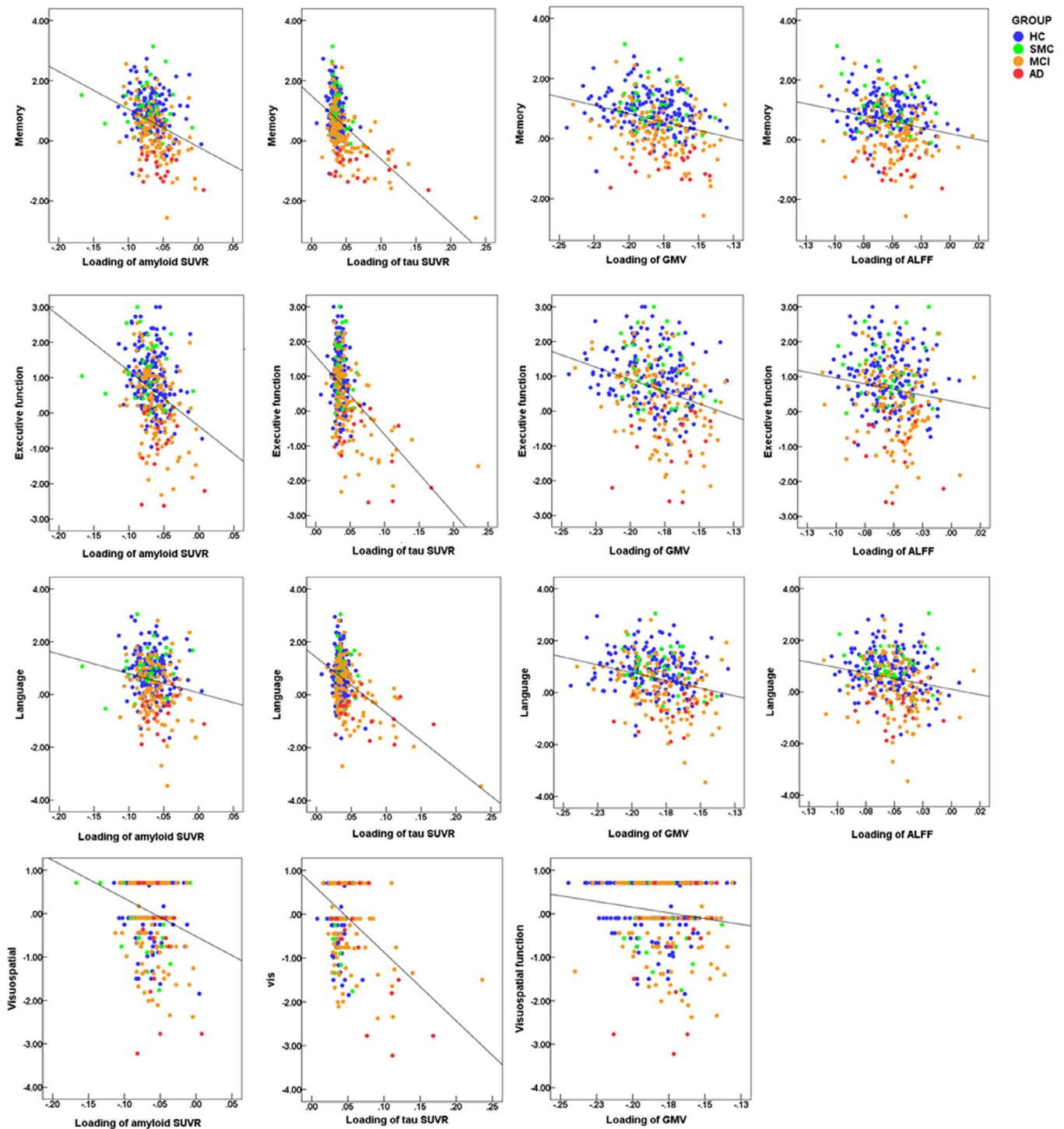
FIGURE 3 Correlations between loadings of the imaging features and cognitive scores in all subjects. AD, Alzheimer's disease; ALFF, amplitude of low frequency fluctuations; MCI, mild cognitive impairment; HC, healthy control; SMC, subjective memory complaint; SUVR, standard uptake value ratios

Similar to the multimodal pattern associated with NPS total score, several common changes were observed in the subcortical, temporal, and parietal regions. Notably, subsyndrome-specific multimodal patterns were also identified, especially in the sensor-motor (SM) and occipital regions. Thereinto, SM showed increased GMV or ALFF with or without regional AD pathology deposition,

while occipital changes are less consistent in different subsyndromes.

To show the multimodal brain alterations more clearly, we summarize all the results into Figure 5 to show the NPS associated co-occurring patterns. We performed additional analyses to prove the robustness of our findings: (1) to reduce the possible effect of age,

TABLE 3 Results of multiple regression analyses using the stepwise variable selection method

	β-coefficient[a]	p-Value
Annual change rate of ADNI_MEM, adjusted R^2 = .108, p < .001		
loading of Tau SUVR	−.243	.000
loading of GMV	−.217	.002
Annual change rate of ADNI_EF, adjusted R^2 = .040, p = .007		
loading of Tau SUVR	.145	.039
loading of GMV	−.185	.009
Annual change rate of ADNI_LAN, adjusted R^2 = .046, p = .001		
loading of Amyloid SUVR	−.226	.001

Abbreviations: AD, Alzheimer's disease; ADNI-EF, the composite scores for executive function in ADNI; ADNI-LAN, the composite scores for language in ADNI; ADNI-MEM, the composite scores for memory in ADNI; ADNI-VS, the composite scores for visuospatial function in ADNI; ALFF, amplitude of low frequency fluctuations; GMV, gray matter volume; HC, healthy control; MCI, mild cognitive control; SMC, subjective memory complaint; SUVR, standard uptake value ratios.
[a]Standardized β.

gender, education and sites, we include them as covariates in the ANOVA analysis of group differences (Supplementary Material 11) and associations between imaging features and cognition (Supplementary Material 12); (2) to show the possible effect of data distribution, we transformed the reference data and repeated the fusion analysis (Supplementary Material 13). Results remain largely consistent with our original findings. Details can be found in Supplementary Materials 11–14.

4 | DISCUSSION

We applied a multimodal fusion method and identified an NPS-related multimodal covarying pattern. The loading of this multimodal pattern started to increase from the MCI stage and progressively worsens with the advancement of AD. It was associated with impairments in multiple cognitive domains and had good predictability in longitudinal cognitive decline. Further analysis using the subsyndrome scores as references partially replicated the NPS-related patterns but also revealed some subsyndrome-specific patterns. Collectively, the current study provided insights into the linkage between NPS and multimodal brain alterations in AD, which might underpin the disease onset and progression.

4.1 | NPS associated multimodal pattern spatially involves frontal-subcortical limbic circuits, which significantly associated with cognitive performance and progression

A pathological–structural–functional covaried pattern was observed in the HP, thalamus, caudate, IPL, and frontal regions. These regions

are core components of the frontal-subcortical limbic circuit (Chen et al., 2021), important for emotion regulation and cognitive function. Similarly, based on rsfMRI data alone, Wang et al. also identified the front-limbic regions as the core areas of NPS in AD (Wang et al., 2019).

Functionally, the frontal-subcortical circuit is typically associated with emotional/cognitive integration, while the IPL–subcortical circuit is associated with sensory/cognitive integration. For example, disturbances in the frontal regions can cause attentional and cognitive disturbances, and subcortical regions are associated with insomnia and loss of appetite (Chen et al., 2021). Moreover, hippocampal-prefrontal cortex dysconnectivity has been found associated with cognitive dysfunction in both major depression and AD (Sampath et al., 2017). Therefore, impairment of the frontal-subcortical limbic circuit may contribute to both cognitive decline and concomitant NPS in AD patients.

Our results provide additional insights. To be specific, group comparisons showed progressively increased loadings of NPS-associated multimodal patterns along the whole AD continuum, and the multimodal pattern was significantly associated with cognition, including memory, executive, language, and visuospatial function. These results prove that the identified NPS-associated multimodal pattern significantly affects cognition in AD. Notably, baseline multimodal imaging features but not the baseline NPS total score could effectively predict the longitudinal cognitive decline. This indicates that the identified multimodal brain alterations may the potential neural mechanisms underlying the associations between NPS and cognitive decline.

4.2 | Different frontal-subcortical limbic circuit regions suffer different pathogenic mechanisms in AD subjects concomitant with NPS

Our further analysis found significant inter-modal associations and demonstrated the interactions among different complex neuropathologies. Similarly, another study found that the NPS-associated brain circuit identified from rsfMRI can further predict the baseline and longitudinal changes of AD pathology (Wang et al., 2019). Combining the inter-modal associations and spatial information can help us to explore the different pathogenic mechanisms underlying different components of the frontal-subcortical circuit.

To be specific, IPL suffered amyloid deposition and decreased brain function, while the temporal regions suffered Tau deposition and GMV atrophy, indicating that these AD biomarkers were responsible for IPL and temporal degeneration. Similarly, another study also observed the strongest association between Tau and NPS in the temporal regions in the preclinical AD (Pichet Binette et al., 2021). This is consistent with the AD neuropathology spread pattern: amyloid deposition starts from the precuneus/parietal regions while Tau deposition starts from the temporal regions.

Interestingly, functional changes were found in frontal regions without apparent AD pathology. Several possible reasons exist. First, the effect of network modulation may be the key reason. Supporting
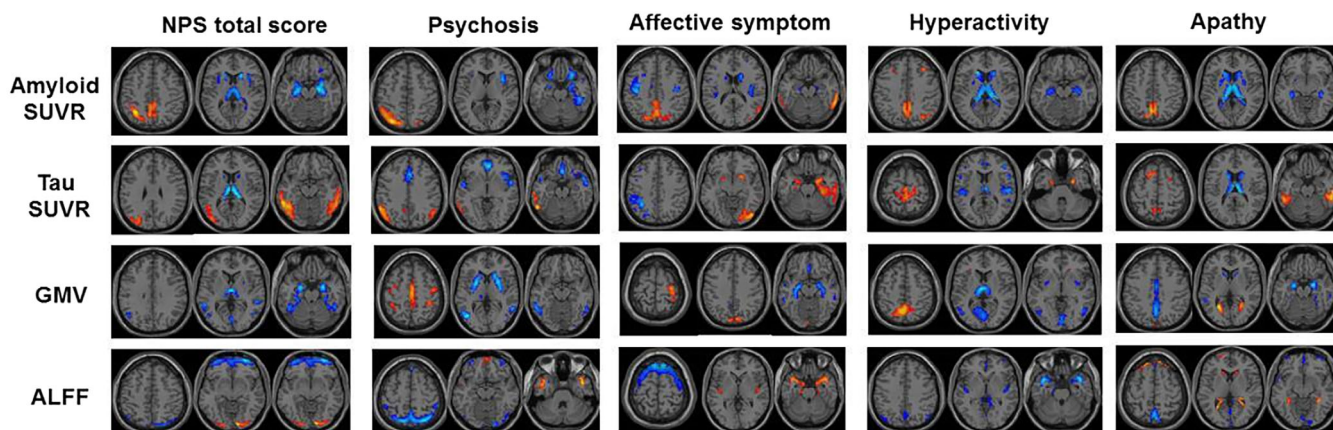
FIGURE 4 The identified joint components using NPS subsyndrome scores as the reference. ALFF, fractional amplitude of low frequency fluctuations; GMV, gray matter volume; NPS, neuropsychiatric symptoms; SUVR, standard uptake value ratios

FIGURE 5 Neuropsychiatric symptoms (NPS) associated multimodal brain regions and their predictivity in the cognitive progression. To summary the results here, the IPL, subcortical regions, HP, and frontal regions work together as the core structures to keep the neuropsychiatric symptoms and cognitive function. Correlation analysis and regression analysis indicate that these regions are significantly correlated with cognition. ALFF, amplitude of low frequency fluctuations; GMV, gray matter volume; HP, hippocampus; ITG, inferior temporal gyrus
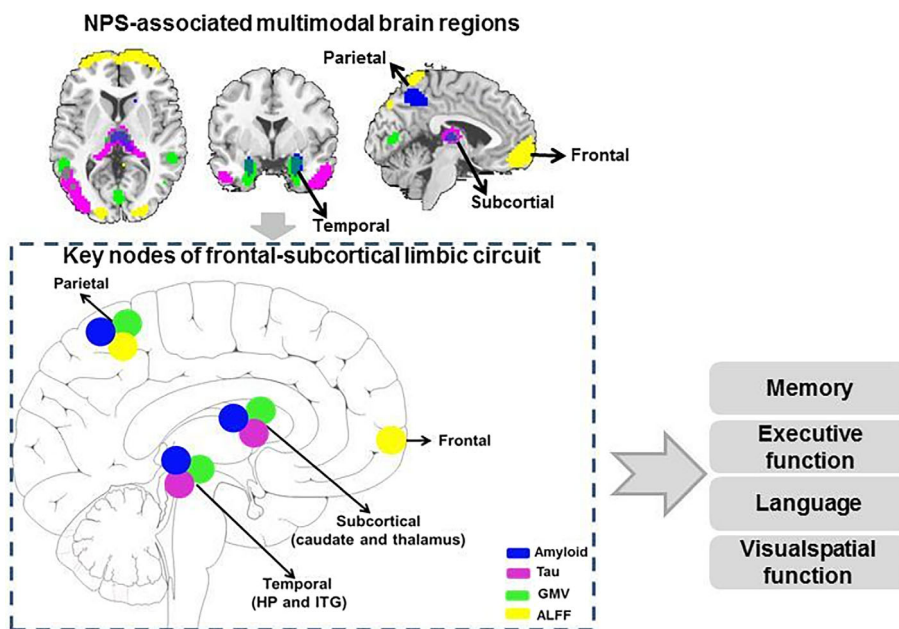
evidence can be obtained from previous studies, which proposed that the frontal is relatively spared from the AD neuropathological deposition while is more initiated as the compensatory mechanism resulted from the network modulation. Moreover, other factors, like genetic and environmental factors, should also be considered. For example, alterations in microRNA-124 in frontal regions are specifically associated with social behavioral deficits and autism (Mor et al., 2015). However, more work needs to be done to clarify this problem.

4.3 | Subsyndrome-specific patterns identified among neuropsychiatric subsyndromes

Variability in neuropsychiatric subsyndromes may be resulted from the disruption of different neural networks in AD. Here,

subsyndrome-specific multimodal patterns were identified, especially in the occipital regions and SM.

The occipital lobe participates in perceiving personal communication and social interactions. Previous studies have reported the association between occipital structures and anxiety/disinhibition (Boublay et al., 2020) and visual hallucinations (Holroyd et al., 2000; Lin et al., 2006). In the current study, the affective symptom is specifically associated with increased Tau deposition and GMV in the occipital regions, indicating the disturbance may be a key pathogenic feature. Interestingly, we also observed the hyperactivity-associated amyloid deposition increase in the frontal regions and ALFF decrease in the occipital regions. Such covariation patterns that involve distinct brain regions may be the results of system modulation.

SM has been found connected with the emotion circuit and associated with NPS in AD (Chen et al., 2021), for example, depression and anxiety (Boublay et al., 2020). In the current study, psychosis and

affective symptom are associated with increased GMV in the SM regions, while hyperactivity is associated with increased Tau deposition and ALFF in the SM regions. The possible explanation is that SM is the transfer hub which conveys the sensory information contained from the emotion-inducing stimuli to other brain regions.

4.4 | The possible connective mechanism between NPSs and AD neuropathology

There are several possible connective mechanisms between NPSs and AD neuropathology. One is that NPSs may arise because of AD neuropathology. That is, AD neuropathology affects key brain regions of underlying emotional, mental and cognitive, so NPSs may be the non-cognitive manifestation of AD (Jicha & Carr, 2010). Alternatively, NPS may be the causal reason which affects circuit function and finally lead to accelerated cognitive impairment. Furthermore, NPSs and AD neuropathology may co-occur because of some shared pathologic processes, such as brain vascular disease or WM change (Alexopoulos, 2006), or the shared genetic factors, like apolipoprotein E (Porcelli et al., 2016; Ye et al., 2016). In this case, there is no causal relationship between NPSs and AD neuropathology but rather is a third factor.

5 | LIMITATION

There are several limitations to the current study. First, the sample sizes of different groups are unbalanced, with a relatively small sample size for the AD group. Future studies with balanced subjects for each group should be validated. Second, the intrinsic causality between the four features may provide further information about the underlying interaction. The current study is mainly descriptive and needs further investigation. Finally, the possible connective mechanism between NPSs and AD neuropathology is not clear. Further study should focus more on this question.

6 | CONCLUSION

NPS was associated with a multimodal imaging pattern involving complex neuropathologies. This pattern was correlated with cognitive performance and could predict cognitive decline. This evidence highlights the importance of NPS in AD progression and may provide clues for future treatment studies or for clinical management.

AUTHOR CONTRIBUTIONS
Kaicheng Li and Qingze Zeng contributed equally to this work. Kaicheng Li designed the study and wrote the first draft of the manuscript, analyzed the MRI data and wrote the protocol. Qingze Zeng collected clinical and MRI data. Xiao Luo, Peiyu Huang, Minming Zhang, Yanxing Chen, Zheyu Li, Yanv Fu, Zhirong Liu, Xiaocao Liu, Luwei Hong, and Vince D. Calhoun assisted with study design and interpretation of findings. Xiaopei Xu, Zening Fu, and Shile Qi modified the expression and grammar thoroughly. All authors have contributed to and approved the final manuscript. All authors read and approved the final manuscript.

ORCID
Shile Qi https://orcid.org/0000-0003-3486-2277
Zening Fu https://orcid.org/0000-0002-1591-4900
Yanxing Chen https://orcid.org/0000-0002-8571-2802
Peiyu Huang https://orcid.org/0000-0003-4226-9369
Minming Zhang https://orcid.org/0000-0003-0145-7558

REFERENCES
Aalten, P., Verhey, F. R., Boziki, M., Bullock, R., Byrne, E. J., Camus, V., Caputo, M., Collins, D., De Deyn, P. P., Elina, K., Frisoni, G., Girtler, N., Holmes, C., Hurt, C., Marriott, A., Mecocci, P., Nobili, F., Ousset, P. J., Reynish, E., ... Robert, P. H. (2007). Neuropsychiatric syndromes in dementia. Results from the European Alzheimer disease consortium: Part I. *Dementia and Geriatric Cognitive Disorders*, *24*(6), 457–463.

Alexopoulos, G. S. (2006). The vascular depression hypothesis: 10 years later. *Biological Psychiatry*, *60*(12), 1304–1305.

Ballarini, T., Iaccarino, L., Magnani, G., Ayakta, N., Miller, B. L., Jagust, W. J., Gorno-Tempini, M. L., Rabinovici, G. D., & Perani, D. (2016). Neuropsychiatric subsyndromes and brain metabolic network dysfunctions in early onset Alzheimer's disease. *Human Brain Mapping*, *37*(12), 4234–4247.

Boublay, N., Bouet, R., Dorey, J. M., Padovan, C., Makaroff, Z., Fédérico, D., Gallice, I., Barrellon, M. O., Robert, P., Moreaud, O., Rouch, I., Krolak-Salmon, P. Alzheimer's Disease Neuroimaging Initiative. (2020). Brain volume predicts behavioral and psychological symptoms in Alzheimer's disease. *Journal of Alzheimer's Disease*, *73*(4), 1343–1353.

Buckner, R. L., Andrews-Hanna, J. R., & Schacter, D. L. (2008). The brain's default network: Anatomy, function, and relevance to disease. *Annals of the New York Academy of Sciences*, *1124*, 1–38.

Buckner, R. L., Snyder, A. Z., Shannon, B. J., LaRossa, G., Sachs, R., Fotenos, A. F., Sheline, Y. I., Klunk, W. E., Mathis, C. A., Morris, J. C., & Mintun, M. A. (2005). Molecular, structural, and functional characterization of Alzheimer's disease: Evidence for a relationship between default activity, amyloid, and memory. *The Journal of Neuroscience*, *25*, 7709–7717.

Chao-Gan, Y., & Yu-Feng, Z. (2010). DPARSF: A MATLAB toolbox for "pipeline" data analysis of resting-state fMRI. *Frontiers in Systems Neuroscience*, *4*, 13.

Chen, Y., Dang, M., & Zhang, Z. (2021). Brain mechanisms underlying neuropsychiatric symptoms in Alzheimer's disease: A systematic review of

symptom-general and -specific lesion patterns. *Molecular Neurodegeneration*, 16(1), 38.

Cuadra, M. B., Cammoun, L., Butz, T., Cuisenaire, O., & Thiran, J. P. (2005). Comparison and validation of tissue modelization and statistical classification methods in T1-weighted MR brain images. *IEEE Transactions on Medical Imaging*, 24(12), 1548–1565.

Cummings, J. L. (1997). The neuropsychiatric inventory: Assessing psychopathology in dementia patients. *Neurology*, 48(5 Suppl 6), S10–S16.

Ehrenberg, A. J., Suemoto, C. K., França Resende, E. P., Petersen, C., Leite, R. E. P., Rodriguez, R. D., Ferretti-Rebustini, R. E. L., You, M., Oh, J., Nitrini, R., Pasqualucci, C. A., Jacob-Filho, W., Kramer, J. H., Gatchel, J. R., & Grinberg, L. T. (2018). Neuropathologic correlates of psychiatric symptoms in Alzheimer's disease. *Journal of Alzheimer's Disease*, 66(1), 115–126.

Fischer, C. E., Ismail, Z., & Schweizer, T. A. (2012). Delusions increase functional impairment in Alzheimer's disease. *Dementia and Geriatric Cognitive Disorders*, 33(6), 393–399.

Friston, K. J., Williams, S., Howard, R., Frackowiak, R. S., & Turner, R. (1996). Movement-related effects in fMRI time-series. *Magnetic Resonance in Medicine*, 35(3), 346–355.

Gonzalez-Escamilla, G., Lange, C., Teipel, S., Buchert, R., Grothe, M. J., & Alzheimer's Disease Neuroimaging Initiative. (2017). PETPVE12: An SPM toolbox for partial volume effects correction in brain PET—Application to amyloid imaging with AV45-PET. *NeuroImage*, 147, 669–677.

Holroyd, S., Shepherd, M. L., & Downs, J. H., 3rd. (2000). Occipital atrophy is associated with visual hallucinations in Alzheimer's disease. *The Journal of Neuropsychiatry and Clinical Neurosciences*, 12(1), 25–28.

Jicha, G. A., & Carr, S. A. (2010). Conceptual evolution in Alzheimer's disease: Implications for understanding the clinical phenotype of progressive neurodegenerative disease. *Journal of Alzheimer's Disease*, 19(1), 253–272.

Karttunen, K., Karppi, P., Hiltunen, A., Vanhanen, M., Välimäki, T., Martikainen, J., Valtonen, H., Sivenius, J., Soininen, H., Hartikainen, S., Suhonen, J., Pirttilä, T., & for the ALSOVA study group. (2011). Neuropsychiatric symptoms and quality of life in patients with very mild and mild Alzheimer's disease. *International Journal of Geriatric Psychiatry*, 26(5), 473–482.

Krell-Roesch, J., Vassilaki, M., Mielke, M. M., Kremers, W. K., Lowe, V. J., Vemuri, P., Machulda, M. M., Christianson, T. J., Syrjanen, J. A., Stokin, G. B., Butler, L. M., Traber, M., Jack, C. R., Jr., Knopman, D. S., Roberts, R. O., Petersen, R. C., & Geda, Y. E. (2019). Cortical β-amyloid burden, neuropsychiatric symptoms, and cognitive status: The Mayo Clinic Study of Aging. *Translational Psychiatry*, 9(1), 123.

Kvavilashvili, L., Niedźwieńska, A., Gilbert, S. J., & Markostamou, I. (2020). Deficits in spontaneous cognition as an early marker of Alzheimer's disease. *Trends in Cognitive Sciences*, 24(4), 285–301.

Li, Y. O., Adali, T., & Calhoun, V. D. (2007). Estimating the number of independent components for functional magnetic resonance imaging data. *Human Brain Mapping*, 28(11), 1251–1266.

Lin, S. H., Yu, C. Y., & Pai, M. C. (2006). The occipital white matter lesions in Alzheimer's disease patients with visual hallucinations. *Clinical Imaging*, 30(6), 388–393.

Lyketsos, C. G., Carrillo, M. C., Ryan, J. M., Khachaturian, A. S., Trzepacz, P., Amatniek, J., Cedarbaum, J., Brashear, R., & Miller, D. S. (2011). Neuropsychiatric symptoms in Alzheimer's disease. *Alzheimer's & Dementia*, 7(5), 532–539.

Lyketsos, C. G., Lopez, O., Jones, B., Fitzpatrick, A. L., Breitner, J., & DeKosky, S. (2002). Prevalence of neuropsychiatric symptoms in dementia and mild cognitive impairment: Results from the cardiovascular health study. *Journal of the American Medical Association*, 288(12), 1475–1483.

Mor, M., Nardone, S., Sams, D. S., & Elliott, E. (2015). Hypomethylation of miR-142 promoter and upregulation of microRNAs that target the oxytocin receptor gene in the autism prefrontal cortex. *Molecular Autism*, 6, 46.

Mormino, E. C., Smiljic, A., Hayenga, A. O., Onami, S. H., Greicius, M. D., Rabinovici, G. D., Janabi, M., Baker, S. L., Yen, I. V., Madison, C. M., Miller, B. L., & Jagust, W. J. (2011). Relationships between β-amyloid and functional connectivity in different components of the default mode network in aging. *Cerebral Cortex*, 21(10), 2399–2407.

Muller-Gartner, H. W., Links, J. M., Prince, J. L., Bryan, R. N., McVeigh, E., Leal, J. P., Davatzikos, C., & Frost, J. J. (1992). Measurement of radiotracer concentration in brain gray matter using positron emission tomography: MRI-based correction for partial volume effects. *Journal of Cerebral Blood Flow and Metabolism*, 12, 571–583.

Peters, M. E., Schwartz, S., Han, D., Rabins, P. V., Steinberg, M., Tschanz, J. T., & Lyketsos, C. G. (2015). Neuropsychiatric symptoms as predictors of progression to severe Alzheimer's dementia and death: The Cache County Dementia Progression Study. *The American Journal of Psychiatry*, 172(5), 460–465.

Pichet Binette, A., Vachon-Presseau, É., Morris, J., Bateman, R., Benzinger, T., Collins, D. L., Poirier, J., Breitner, J. C. S., Villeneuve, S., Allegri, R., Amtashar, F., Bateman, R., Benzinger, T., Berman, S., Bodge, C., Brandon, S., Brooks, W. (. B.)., Buck, J., Buckles, V., … Bedetti, C. (2021). Amyloid and tau pathology associations with personality traits, neuropsychiatric symptoms, and cognitive lifestyle in the preclinical phases of sporadic and autosomal dominant Alzheimer's disease. *Biological Psychiatry*, 89(8), 776–785.

Porcelli, S., Crisafulli, C., Donato, L., Calabrò, M., Politis, A., Liappas, I., Albani, D., Atti, A. R., Salfi, R., Raimondi, I., Forloni, G., Papadimitriou, G. N., de Ronchi, D., & Serretti, A. (2016). Role of neurodevelopment involved genes in psychiatric comorbidities and modulation of inflammatory processes in Alzheimer's disease. *Journal of the Neurological Sciences*, 370, 162–166.

Power, J. D., Barnes, K. A., Snyder, A. Z., Schlaggar, B. L., & Petersen, S. E. (2012). Spurious but systematic correlations in functional connectivity MRI networks arise from subject motion. *NeuroImage*, 59(3), 2142–2154.

Qi, S., Abbott, C. C., Narr, K. L., Jiang, R., Upston, J., McClintock, S. M., Espinoza, R., Jones, T., Zhi, D., Sun, H., Yang, X., Sui, J., & Calhoun, V. D. (2020). Electroconvulsive therapy treatment responsive multimodal brain networks. *Human Brain Mapping*, 41(7), 1775–1785.

Qi, S., Calhoun, V. D., van Erp, T. G. M., Bustillo, J., Damaraju, E., Turner, J. A., du, Y., Yang, J., Chen, J., Yu, Q., Mathalon, D. H., Ford, J. M., Voyvodic, J., Mueller, B. A., Belger, A., McEwen, S., Potkin, S. G., Preda, A., Jiang, T., & Sui, J. (2018). Multimodal fusion with reference: Searching for joint neuromarkers of working memory deficits in schizophrenia. *IEEE Transactions on Medical Imaging*, 37(1), 93–105.

Sampath, D., Sathyanesan, M., & Newton, S. S. (2017). Cognitive dysfunction in major depression and Alzheimer's disease is associated with hippocampal-prefrontal cortex dysconnectivity. *Neuropsychiatric Disease and Treatment*, 13, 1509–1519.

Scaricamazza, E., Colonna, I., Sancesario, G. M., Assogna, F., Orfei, M. D., Franchini, F., Sancesario, G., Mercuri, N. B., & Liguori, C. (2019). Neuropsychiatric symptoms differently affect mild cognitive impairment and Alzheimer's disease patients: A retrospective observational study. *Neurological Sciences*, 40(7), 1377–1382.

Sui, J., Qi, S., van Erp, T. G. M., Bustillo, J., Jiang, R., Lin, D., Turner, J. A., Damaraju, E., Mayer, A. R., Cui, Y., Fu, Z., Du, Y., Chen, J., Potkin, S. G., Preda, A., Mathalon, D. H., Ford, J. M., Voyvodic, J., Mueller, B. A., … Calhoun, V. D. (2018). Multimodal neuromarkers in schizophrenia via cognition-guided MRI fusion. *Nature Communications*, 9(1), 3028. https://doi.org/10.1038/s41467-41018-05432-w

Teng, E., Lu, P. H., & Cummings, J. L. (2007). Neuropsychiatric symptoms are associated with progression from mild cognitive impairment to Alzheimer's disease. *Dementia and Geriatric Cognitive Disorders*, 24(4), 253–259.

Tissot, C., Therriault, J., Pascoal, T. A., Chamoun, M., Lussier, F. Z., Savard, M., Mathotaarachchi, S. S., Benedet, A. L., Thomas, E. M., Parsons, M., Nasreddine, Z., Rosa-Neto, P., & Gauthier, S. (2021).

Association between regional tau pathology and neuropsychiatric symptoms in aging and dementia due to Alzheimer's disease. *Alzheimer's & Dementia, 7*(1), e12154.

Wang, X., Ren, P., Mapstone, M., Conwell, Y., Porsteinsson, A. P., Foxe, J. J., et al. (2019). Identify a shared neural circuit linking multiple neuropsychiatric symptoms with Alzheimer's pathology. *Brain Imaging and Behavior, 13*(1), 53–64.

Ye, Q., Bai, F., & Zhang, Z. (2016). Shared genetic risk factors for late-life depression and Alzheimer's disease. *Journal of Alzheimer's Disease, 52*(1), 1–15.

Zang, Y. F., He, Y., Zhu, C. Z., Cao, Q. J., Sui, M. Q., Liang, M., Tian, L. X., Jiang, T. Z., & Wang, Y. F. (2007). Altered baseline brain activity in children with ADHD revealed by resting-state functional MRI. *Brain & Development, 29*(2), 83–91.

SUPPORTING INFORMATION

Additional supporting information can be found online in the Supporting Information section at the end of this article.

How to cite this article: Li, K., Zeng, Q., Luo, X., Qi, S., Xu, X., Fu, Z., Hong, L., Liu, X., Li, Z., Fu, Y., Chen, Y., Liu, Z., Calhoun, V. D., Huang, P., & Zhang, M. (2023). Neuropsychiatric symptoms associated multimodal brain networks in Alzheimer's disease. *Human Brain Mapping, 44*(1), 119–130. https://doi.org/10.1002/hbm.26051